MICROCHANNEL TOPOLOGY OPTIMIZATION BASED ON ENHANCED HEAT TRANSFER MECHANISM

Wenzhu LIU, Heming YUN*, Baoxue WANG, Mingzhe HU, and Chonglong ZHONG

School of Thermal Engineering, Shandong Jianzhu University, Jinan, 250101, China

*Corresponding author; E-mail: yunheming@163.com

Topology optimization modifies the material distribution in the design domain to produce microchannel structure with improved thermal performance. In this work, five heat dissipation microchannel structures with various design domain aspect ratios are optimally designed based on the bi-objective topology optimization method. The optimal design variable fields, temperature fields, and pressure fields are subsequently obtained for each operating condition, and the flow heat transfer effect and the enhanced heat transfer mechanism are investigated under various working conditions. On this basis, the flow heat transfer impact of microchannels under various operating situations is optimized and studied by combining the field synergy concept and entransy dissipation theory. The findings show that when the Reynolds number rises in the laminar flow region, the complexity of the topological flow channels also rises. The average temperature T_{ave} decreases, Nu rises, the inlet and outlet pressure drop ΔP gradually increases, the integrated enhanced heat transfer factor PEC gradually decreases, the field synergy number F_c increases, the pressure drop synergy angle θ gradually increases, the entransy dissipation E_{vh} increases, and the flow heat transfer performance of each heat dissipation channel is also enhanced due to the complex channels and high Reynolds number in the domain. The investigation of microchannels with various topologies revealed that the microchannels with the same boundary conditions and a design domain aspect ratio of 25/64 had the best synergy effects of velocity-pressure gradient and velocity-temperature gradient, the best heat transfer effect, and the best flow characteristics.

Key words: *Microchannel, Bi-objective optimization, Topology optimization, Field synergy principle, Entransy dissipation theory*

1. Introduction

With the rapid advancement of microelectronics technology, the degree of integration and downsizing of electronic equipment have been increased, as well as its power density. For every 1°C increase in temperature when the temperature of microelectronic devices is between 70°C and 80°C, the reliability and stability will decline by 5% [1]. Therefore, in order to guarantee their good operation and satisfy potentially increasing thermal needs in the future, efficient development of thermal management technologies is required. Tuckermann and Pease [2] first presented a thermal management approach in 1981, which entailed embedding microchannels at the base of an electronic

chip and driving convection through a liquid to remove the excessive heat produced by the chip. Microchannel heat dissipation as an efficient means of heat dissipation technology has great potential for heat dissipation in electronic devices with high heat flow density.

Structural design has been still the most popular approach for improving heat sink performance over the past few decades [3-5]. According to Zhu et al. [6], trapezoidal-grooved microchannels are effective at transferring heat. Fang et al. [7] investigated the way various structural factors of S-type turbulators affected the laminar flow and heat transfer efficiency of rectangular microchannels. In addition, some more complex channels with better overall performance have also been proposed such as double-layered microchannels [8], wavy microchannels [9, 10], fins and hybrid microchannels [11], etc. These type of design methodology, which obviously largely relied on the designer's intuition, might not produce the best microchannel structure and could not be as effective as a non-intuitive design methodology.

Given the optimization objective and boundary conditions, topology optimization is the process of modifying the form of the material distribution in the design domain in order to find the best possible solution to the objective function. Bendse and Kikuchi [12] developed the homogenization approach for continuum topology optimization based on homogenization theory in 1988. Then, the topology optimization method for fluid flow was initially applied by Borrvall and Petersson [13] in 2003, and they proposed a density-based approach to decrease the power lost by the Stokes flow. Since then, the topology optimization approach has been used to resolve numerous flow field optimization issues. For the design of the microchannel structure, Wang et al. [14], Yaji et al. [15], and Xia et al. [16] adopt a dual-objective topology optimization technique that takes into account the two key index values of flow resistance and heat transfer performance. Zhang et al. [17] proposed an interleaved bidirectional flow cooling method with the maximum temperature and maximum temperature difference as the objectives. Zou et al. [18] established a comprehensive technique for the construction of micro heat sinks that enables the direct estimation of the weight parameters.

Despite the fact that the strengthening techniques discussed above have received more attention, they are essentially just upgrades to the technologies already in use and lack some ideas and methods for optimizing heat transport that can boost energy efficiency [19, 20]. In this paper, the finite element method is used to simulate the conjugate heat transfer process of a microchannel heat sink, five heat sinks with different design domain aspect ratios are developed. Meanwhile, the multi-objective optimization model with optimal thermal performance and minimal fluid energy dissipation is established based on the variable density principle, and the best solution leads to the topology of a positive flow channel. On this basis, the effects of different design domain distribution methods and different Reynolds numbers on their temperature and pressure drop are investigated. The enhanced heat transfer effect is then analyzed employing the field synergy principle and entransy dissipation theory to provide a theoretical study for topology optimization design.

2. Description of the design problems

The microchannel heat sink is built up as an axisymmetric structure with a single inlet and two outlets, with the inlet on one side and the outlet on the other, as illustrated in Fig. 1, which also depicts the geometric configuration and boundary conditions that were investigated in this research. The design domain is shown as the blue region, and the axis of symmetry is depicted as the dashed line. The rectangular region $L_1 \times H_1$ serves as the design domain of the heat sink, and the inlet and outlet of

the flow channel have rectangular shapes with $L_2 \times H_2$. The aspect ratio of the design domain is determined by dividing the length L_1 by the width H_1 of the design domain.

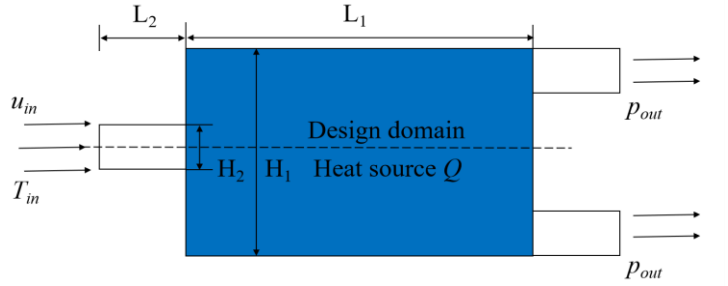

Fig. 1. Geometrical configuration and boundary conditions

In the present work, the inlet fluid with a temperature T_{in} of 293.15K and a velocity u_{in} is introduced; the fluid pressure at the output is set to p_{out}=0; the characteristic length is the inlet length. A constant heat source Q is applied in the design domain. Except for the inlet and outlet and the symmetrical boundary, other walls are adiabatic non-slip boundary. The volume fraction of the fluid material is 0.5 for all cases.

3. Topology optimization models

3.1. Flow model

The design domain is viewed as a porous medium and the steady-state, incompressible, and laminar flow fluid is thought to exist in the microchannel. Due to the flow of fluid has flow resistance in the porous medium, the source of resistance must be included in the fluid-based momentum calculation. The relevant continuity and momentum equation is as follows in order to enable a simulation of the porous domain flow:

$$\nabla \cdot \boldsymbol{u} = 0 \tag{1}$$

$$\rho_f \left(\boldsymbol{u} \cdot \nabla\right)\boldsymbol{u} - \mu_f \nabla^2 \boldsymbol{u} + \nabla p = \boldsymbol{F} \tag{2}$$

where $\boldsymbol{u}$ is the velocity of fluid and ∇ is the gradient operator. ρ_f and μ_f represent the density of fluid and dynamic viscosity of fluid, respectively. p is the pressure of fluid and $\boldsymbol{F}$ stands for the body force term exerted on the fluid by the solid during the optimization process.

According to the Brinkman penalty model, the flow resistance of the porous medium is proportional to the fluid velocity, and $\boldsymbol{F}$ in Eq.(2) is described as follows:

$$\boldsymbol{F} = -\alpha(\gamma)\boldsymbol{u} \tag{3}$$

where α is the inverse permeability of the porous medium. The higher the inverse permeability indicates that it is more challenge for the fluid to flow through the porous media.

Therefore, the flow control equation of the ideal porous medium can be expressed as follows:

$$\rho_f \left(\boldsymbol{u} \cdot \nabla\right)\boldsymbol{u} - \mu_f \nabla^2 \boldsymbol{u} + \nabla p = -\alpha(\gamma)\boldsymbol{u} \tag{4}$$

3.2. Heat transfer model

The power device produces heat in the microchannel heat sink, which is then transported through heat conduction to the solid and liquid regions. If the process is a steady-state heat transfer process, the following heat transfer control equations apply to different microchannel domains:

Fluid domain(γ =1)

$$\rho_f c_p (\boldsymbol{u} \cdot \nabla) T = k_f \nabla^2 T \tag{5}$$

Solid domain(γ =0)

$$k_s \nabla^2 T + Q = 0 \tag{6}$$

where k_f and k_s stand for the thermal conductivities of the fluid and solid parts. c_p is the fixed-pressure specific heat of the fluid. T is the local temperature. Q represents the heat generation per unit volume.

Both the solid and fluid phases exist during the topology optimization process, and the distribution of the fluid and solid domains is unknown. In order to address this problem, Eqs. (5)-(6) can be rewritten into one single equation for the fluid and solid domains, where the design variable γ is used to govern the change of the solid domain and fluid domain in the heat transfer equation [21]:

$$\gamma \rho c_p (\boldsymbol{u} \cdot \nabla) T = \left[(1-\gamma) k_s + \gamma k_f \right] \nabla^2 T + (1-\gamma) Q \tag{7}$$

Assumed is an idealized heat source with temperature, T_Q, where the heat value relates to the change in solid domain temperature. The heat source word Q can therefore be written as follows [22]:

$$Q = h(T_Q - T) \tag{8}$$

where h refers to the heat generation coefficient of the heat source. T is the temperature value at a point in the solid domain.

3.3. Material interpolation model

The most popular of the topological optimization design approaches is the variable density method. It assumes that the distribution of a certain material is controlled by the design variable γ, which varies in a continuous range of 0 to 1. The fluid topology in this work is optimized using the RAMP (Rational Approximation of Material Properties) method [23],which has fewer iterations, higher optimization efficiency, fewer design variables, faster convergence, and the model is more suitable for the study of fluid topology optimization. The RAMP model produces outcomes that are in line with theory, with a more complete and clearer distribution of material and no misleading results. In addition, the RAMP model is designed to penalize topology optimization results that are not 0 or 1, thus effectively reducing the generation of intermediate variables.

The RAMP interpolation formula for the design variable is as follows:

$$\alpha(\gamma) = \alpha_f + (\alpha_s - \alpha_f) q \frac{1-\gamma}{q+\gamma} \tag{9}$$

where γ is the design variable. q is the penalty factor that restrains the median value of design variable. α_f and α_s are the inverse permeability of the fluid and solid domains. The α_s can be expressed as [24]:

$$\alpha_s = \frac{\mu_f}{Da \cdot L^2} \tag{10}$$

where Da is Darcy number and is set as 10^{-4} in this work. μ_f is the dynamic viscosity of fluid and L is the characteristic length.

The thermal conductivity k, density ρ, and specific heat capacity c_p of material are all interpolated here using the RAMP interpolation model and are supplied by [24]:

$$k(\gamma) = k_f + (k_s - k_f) q_k \frac{1-\gamma}{q+\gamma} \tag{11}$$

$$\rho(\gamma) = \rho_f + (\rho_s - \rho_f) q_\rho \frac{1-\gamma}{q+\gamma} \tag{12}$$

$$c_p(\gamma) = c_{p,f} + (c_{p,s} - c_{p,f}) q_{c_p} \frac{1-\gamma}{q+\gamma} \tag{13}$$

where the subscripts *f* and *s* indicate the fluid and solid materials, respectively. q_k, q_ρ, and q_{cp} are the penalty coefficients of the thermal conductivity, density, and specific heat capacity, separately.

3.4. Bi-objective topology optimization

Typically, the heat transfer efficiency and fluid flow energy consumption must be taken into account simultaneously for a thermal management system. In the present study, the fluid objective J_f is to minimize the power dissipation of the fluid during the channel. Inspired by [22], it is adopted in this paper as follows:

$$J_f = \frac{1}{2}\mu \int_\Omega \nabla \boldsymbol{u} \cdot \nabla \boldsymbol{u} d\Omega + \int_\Omega \alpha(\gamma) \boldsymbol{u} \cdot \boldsymbol{u} d\Omega \tag{14}$$

The highest total heat J_{th} in the design domain is used to define the thermal objective function in order to solve the maximizing heat transfer problem, as follows [22]:

$$J_{th} = \int_\Omega (1-\gamma) h (T_Q - T) d\Omega \tag{15}$$

The mobility performance objective and the thermal performance objective are normalized using the weighting coefficient ω, which is then weighted to incorporate them into the objective function of the multi-objective optimization problem. Thus, the minimal total goal *J* is shown as follows:

$$J = (1-\omega) J_f - \omega J_{th} \tag{16}$$

where ω is the weight coefficient of the thermal property. The minus sign in front of J_{th} means that it must be maximized [16].

In conclusion, using the above formulated objective function, the topology optimization problem can be summarized as:

$$\begin{aligned} &Find\ \gamma \\ &Min\ \ J = (1-\omega) J_f - \omega J_{th} \\ &S.t.\quad \int_\Omega \gamma d\Omega \le V_f \\ &\qquad 0 \le \gamma \le 1 \end{aligned} \tag{17}$$

where Ω represents the design domain. V_f is the upper limit of fluid volume fraction.

3.5. Filtering and projection

In topological optimization, numerical instabilities like tessellation lattice and grid dependency are frequent issues. Filters can be adopted to resolve the maladjustment of the optimization problem. In the filtering approach, the Helmholtz differential equation is frequently employed for topology optimization [25] and is formulated as follows:

$$\bar{\gamma} = R_{\min}^2 \nabla^2 \gamma + \gamma \tag{18}$$

where $\bar{\gamma}$ is the filtered design variable and γ is the design variable before filtering. R_{min} is the

filtration radius. The filter radius in this article is set to 1.5 times the mesh size.

The filtration technique described above also can produce a lot of gray scale units between the fluid and the solid material. Therefore, it can be reduced by using the hyperbolic tangent projection to sharpen the border between the fluid and solid domains and address the gray scale problem:

$$\overline{\overline{\gamma}} = \frac{\tanh\left(\beta\left(\overline{\gamma} - \gamma_\beta\right)\right) + \tanh\left(\beta\gamma_\beta\right)}{\tanh\left(\beta\left(1 - \gamma_\beta\right)\right) + \tanh\left(\beta\gamma_\beta\right)} \tag{19}$$

where $\overline{\overline{\gamma}}$ is the new design variable after the projection, which will replace the original variable γ. γ_β and β represent the projection point and the projection slope, individually. In this paper, γ_β is set to 0.5 and β is set to 8.

4. Mesh test and model validation

4.1. Mesh independence test

Mesh independence testing of the design model is necessary to guarantee the precision of the calculation results. A heat sink channel structure with a design domain aspect ratio of 1 was chosen as an example when the Reynolds number is 75. Various numbers of free quadrilateral meshes were adopted to discretize the design domain, with the mesh numbers being 1953, 2956, 5157, 13184, 20941, and 36885, respectively. As seen in Fig. 2, the objective function value J gradually decreases as the number of grids grows, but when the number of grids exceeds 13184, the objective function value stabilizes around 0.75. In this article, the ensuing numerical simulation analysis is performed using a grid number of 13184 while taking into account the computing accuracy and speed.

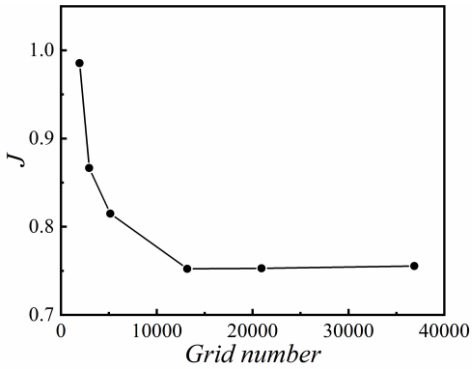

Fig. 2. Correlation plot of objective function value and grid number

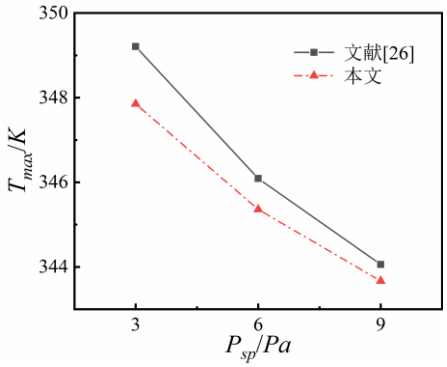

Fig. 3. Comparison of the maximum temperature T_{max} with the specified pressure P_{sp}

4.2. Model validation

In the process of numerical simulation, the validation of the calculation methods adopted in the paper is a critical step to achieve accurate analysis. Thus, the working condition in the literature [26] is estimated for a heat sink inlet velocity of 0.05 m/s and specified pressures of 3, 6, and 9, respectively, in the current investigation. The strategy utilized in this work is then put to the test by adopting the same boundary conditions and presumptions as those in the literature. The calculation approach in this article is deemed reliable since, as shown in Fig. 3, the highest temperature T_{max} in this work and that in the literature [26] differ by 0.39%, 0.21%, and 0.11% in that order.

5. Solution method

In this work, finite element software is chosen to address the aforementioned topology optimization issue. In order to make the discretization design domain easier, the design area and

boundary conditions of the fluid topological structure are first determined. Following the addition of the objective function and restrictions, the sensitivity is determined using the continuous concomitant formula. The design variable is then updated using the sequential quadratic optimization solver (SNOPT) in accordance with the findings of the sensitivity analysis, and a fresh set of design variable values γ is obtained at the end of each iteration to serve as the starting point for the subsequent iteration. If the optimization tolerance of the solver is smaller than 10^{-10}, the optimization procedure is regarded as having converged.

6. Topological results and comparison

6.1. Selection of the weight coefficient

The design objective of this paper is to maximize the heat transfer performance of the fluid in the design domain while minimizing the power dissipation of the fluid flow. Thus, to be able to balance the fluid heat transfer and flow dissipation in accordance with the design requirements, the weight coefficient ω must be carefully chosen in the optimization process. The design domain aspect ratios of 25/64, 16/25, 1, 25/16, and 64/25 are taken to further confirm the precision of the multi-objective topology optimization approach. The topology optimization results of the microchannel structure with five different aspect ratios under different weighting factors are solved, and the distributions of the topological morphology (upper part) and temperature field (lower part) are shown in Fig. 4. The color labels in the figure have scale values of γ and T (in K), respectively. In the diagram, the solid domain is represented by the black, while the fluid domain is depicted by the white.

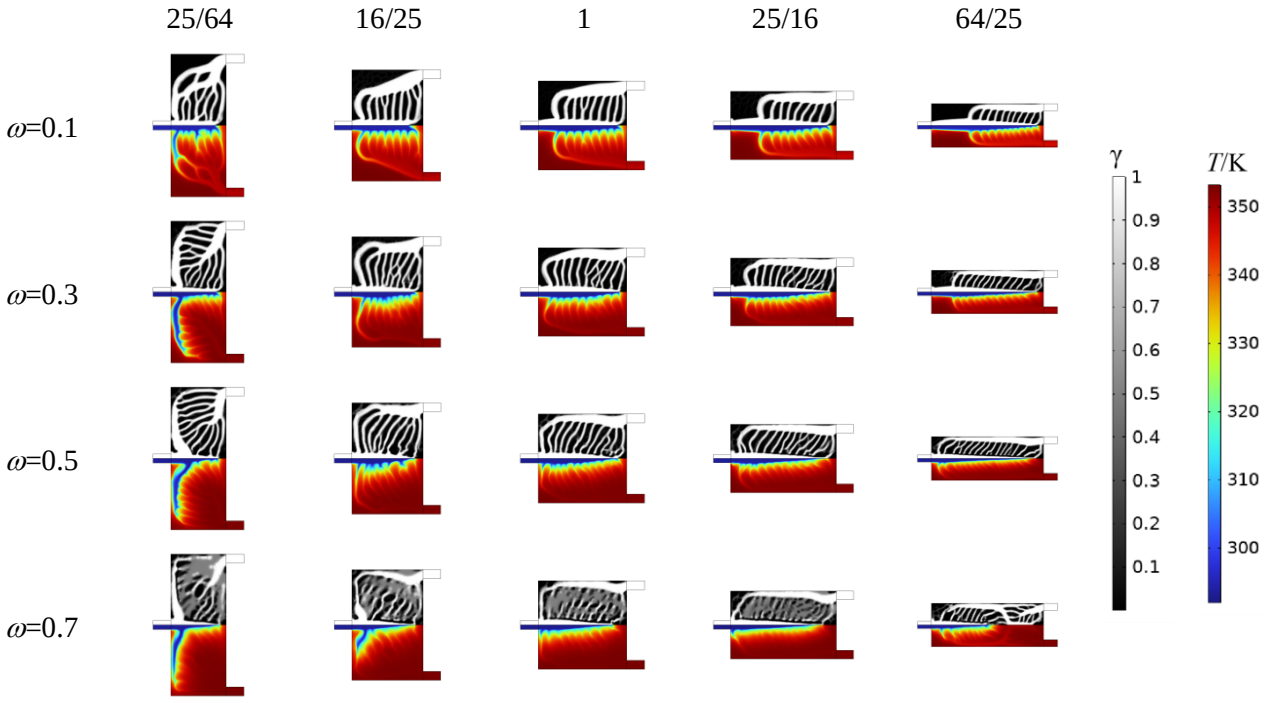

Fig. 4. Optimized design variable and temperature fields of microchannels with different ω

As seen in Fig. 4, when the pressure drop target is assumed to be the dominant control optimization outcome and the weight coefficient ω of the thermal target is taken to be small, the topological channel structure obtained is simple and smooth, the number of flow channel branches is small, and the flow channel size is large, which can significantly reduce the pressure drop loss in the flow channel. When the weight coefficient ω of the thermal target is assumed to be higher, the larger heat exchange boundary is required to exchange heat because the thermal target dominates the

optimization algorithm. As a result, as the weight coefficient rises, the number of flow channels keeps growing and more and more fine branches emerge from the main flow channels, while the flow channels gradually spread over the entire design domain, preventing heat from accumulating in the solid domain.

The increased flow resistance is at the expense of the improved thermal performances [16]. The topology result of the flow channel is too complex, the width of the flow channel is narrow, the path is broken, and the pressure drop in the microchannel is significant as a result of the high weighting coefficient. It is challenging to confirm the accuracy of the results in these circumstances since there will be a significant amount of inaccuracy in the actual engineering and manufacturing. In this regard, the weighting factor of 0.5 is chosen in the topology optimization calculation procedure in this research to assure the temperature homogeneity throughout the design domain.

6.2. Influence of the Reynolds number

In this section, Reynolds number is selected for laminar flow, to explore the impact of various aspect ratio microchannel constructions with varying Reynolds numbers on their temperature and pressure drop at the weighting factor ω of 0.5 and the fluid volume ratio of 0.5.

6.2.1 Analysis of the temperature field characteristics

The distribution of the topological morphology (upper part) and the temperature field (lower part) of the microchannel at different Reynolds number are shown in Fig. 5. The scale values of the color legends in the figure are γ and T (in K), respectively.

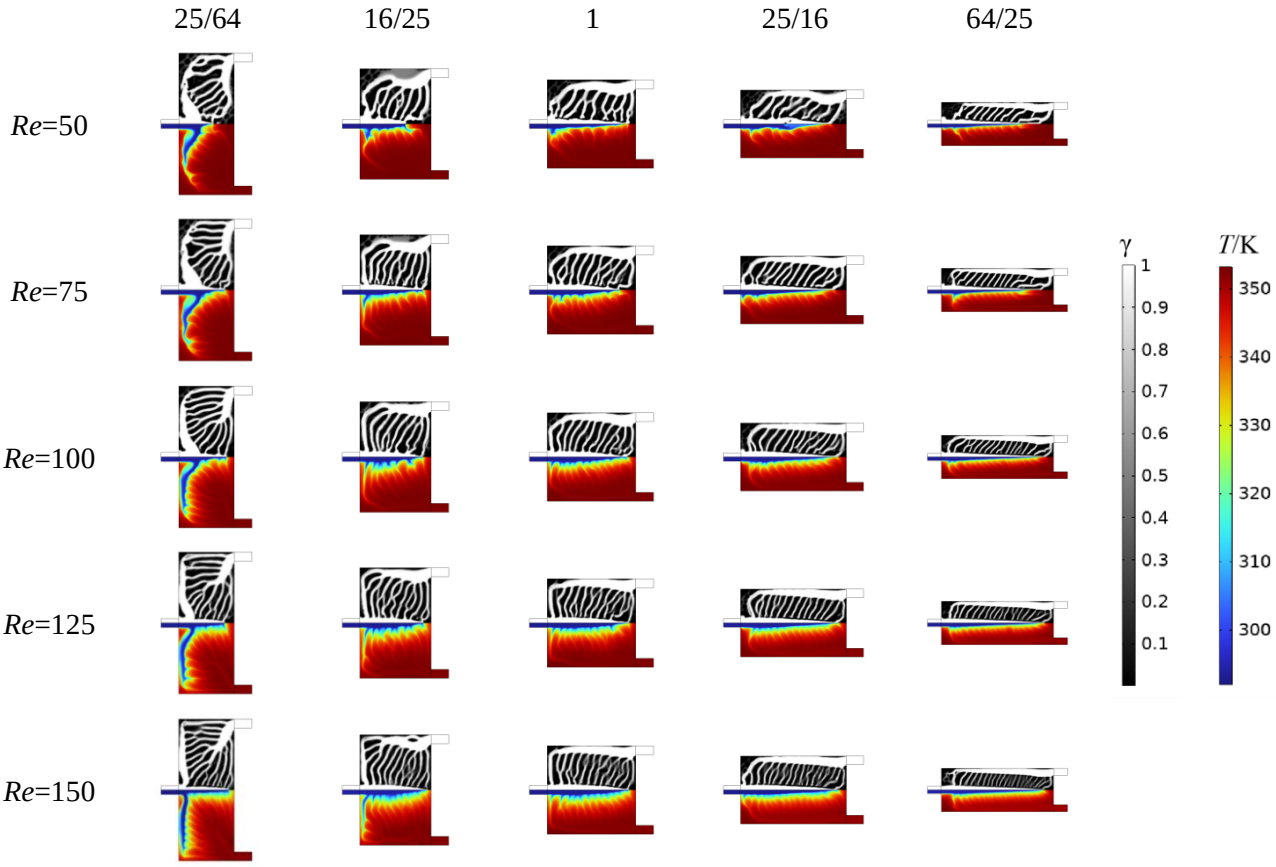

Fig. 5. Variable and temperature fields of microchannel optimized design at different *Re*

According to Fig. 5, it is obvious that as the Reynolds number rises, the topology-optimized

design will have more channels overall, a narrower flow path, and gradually more finely branched flow paths will cover the whole design area. At small Reynolds numbers, the flow path mainly changes in the middle of the design domain, and as the Reynolds number increases, the rear of the design domain becomes more crowded with branches. The distribution of the branches is more uniform the higher the Reynolds number, which causes a steady decrease in the temperature in the design domain and a progressive tendency for the temperature distribution to be uniform. The fine branching flow routes are formed at the channel entrance end and extend towards the back of the design domain for heat dissipation channels with aspect ratios less than 1, with a prominent bow at the entrance and exit; while fine branching flow paths are formed away from the inlet end for narrower heat dissipation channels with aspect ratios greater than 1, the number of fine flow paths increases further as the Reynolds number increases, with the gray area being caused by numerical instability. Overall, the topological flow channel complexity rises with the Reynolds number, which is consistent with the results reported in the literature [22, 27].

In Fig. 6, the relationship between the Reynolds number and the change of average temperature T_{ave} for microchannels with various topological topologies is plotted. It can be seen that with the increase of Reynolds number, the average temperature T_{ave} of the channel gradually decreases, indicating that as Reynolds number rises, the inlet flow rate will be raised, the mass flow rate of fluid can be added, the convective heat transfer coefficient of fluid will be increased, and the heat transfer effect will be enhanced. At the same Reynolds number, the T_{ave} of the five microchannels are increased sequentially with the increase of aspect ratio, which is caused by the enlargement of aspect ratio, the generation of fine branches in the design domain is gradually delayed. Under these circumstances, the narrow flow channel cannot be adequately covered in the design domain, which reduces the contact area between the flow channel and the solid and decreases the area available for heat transfer. This means that the microchannel with the design domain aspect ratio of 25/64 has the superior heat transmission properties since its average temperature is less than that of the other four microchannels.

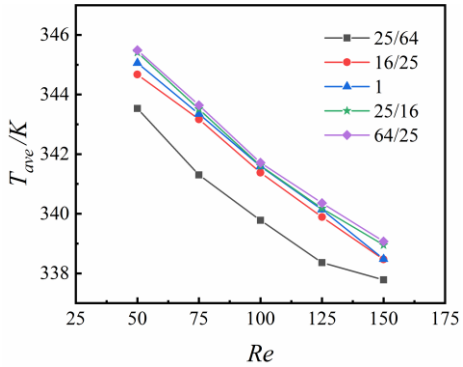

Fig. 6. T_{ave} of microchannels at different *Re*

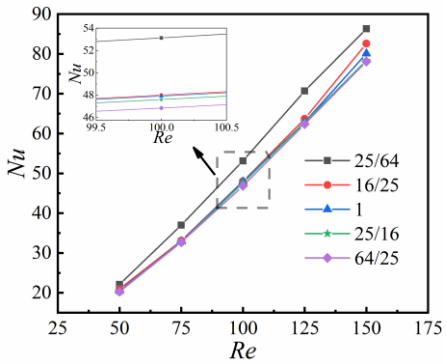

Fig. 7. Nu of the microchannels at different *Re*

Fig. 7 shows the relationship between topological microchannel Nu and Reynolds number for various design domain aspect ratios. Due to the mass flow rate of the fluid increases with Reynolds number, the convective heat transfer coefficient rises and the heat transfer impact is strengthened. As a result, the Nu of various microchannel forms exhibits a rising trend with increasing Reynolds number. The Nu of the microchannel with the aspect ratio of 25/64 is the biggest under the same Reynolds number condition. Since the Nu can accurately describe how well a heat exchanger transfers heat, it is obvious that the microchannel with a 25/64 aspect ratio has the best heat transfer capabilities.

6.2.2 Analysis of the pressure field characteristics

There is the significant pressure loss in the flow field of the microchannel after shunting. Additionally, the distribution of the topological morphology (upper part) and pressure field (lower part) of the heat sink channels with various aspect ratios is illustrated in Fig. 8. The color labels in the figure have scale values of γ and P (in Pa), accordingly.

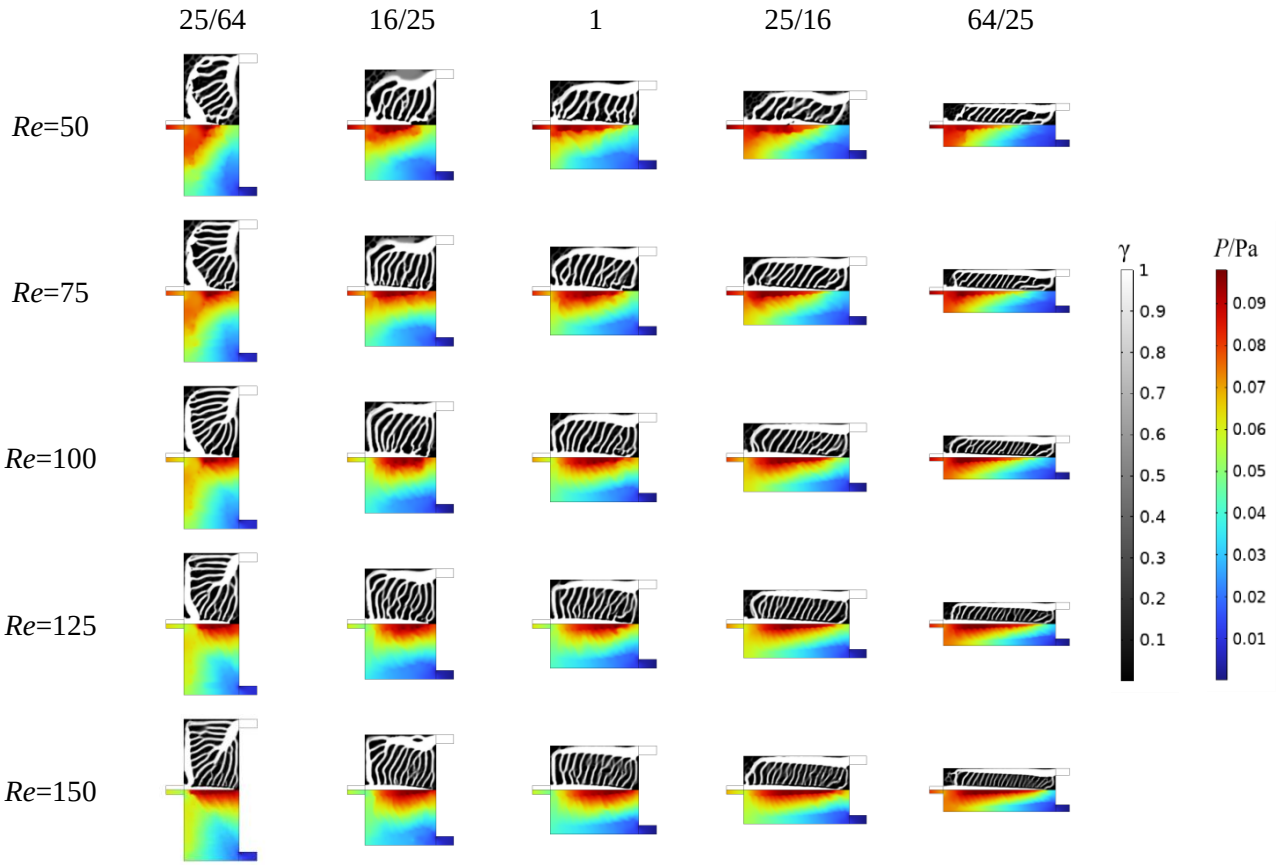

Fig. 8. Variable and pressure fields of microchannel optimized design at different *Re*

The channel pressures in Fig. 8 are all greater at the inlet and less so at the outlet. At the small Reynolds number, the high local flow velocity and the diversion impact of the combined cause of the disturbance result in a fast increase in fluid pressure near the inlet mid-axis and branch diversion. The site of the pressure maximum generation gradually moves to the back of the design domain as the Reynolds number rises, with the channel fluid pressure being bigger at the inner runner and smaller at the outer runner. The reason for such phenomenon is that the inner channel and the back of the design domain are becoming shorter and narrower, and the fluid flow path direction is changing more quickly, which increases the pressure at which the fluid will collide with the solid. The flatter the channel, the greater the fluid flow velocity; the flow resistance is raised and flow characteristics are weakened when the fluid inlet flow is constant under the same Reynolds number, resulting in the inlet and outlet pressure difference increasing gradually with the increase in aspect ratio.

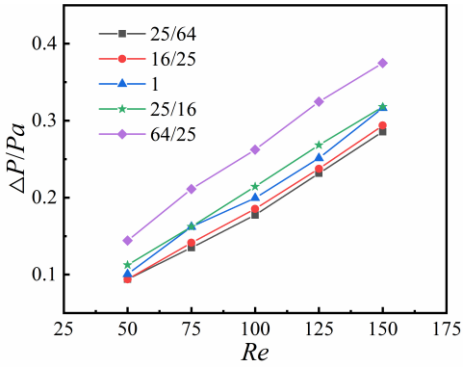

Fig. 9. ΔP of the microchannels at different *Re*

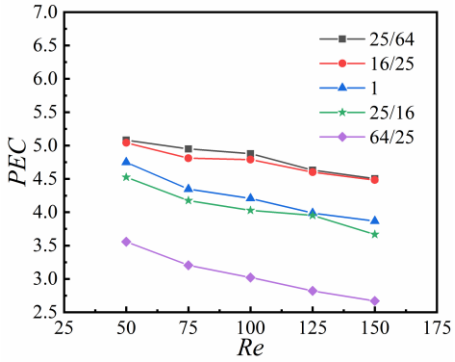

Fig. 10. PEC of the microchannels at different *Re*

The correlation diagram of the microchannel inlet and outlet pressure drop ΔP with different design fields is shown in Fig. 9. As the Reynolds number steadily rises, ΔP gradually rises as well, as can be observed. When the aspect ratio rises, the distribution of fine flow channels is more dense, the channel length decreases so that the direction of the flow channel per unit length changes more quickly, the fluid and wall impact to strengthen the local flow resistance is increased, making the inlet and outlet pressure drops ΔP for microchannels gradually higher under the same Reynolds number. The findings demonstrate that in the design domain, microchannels with larger aspect ratios have higher ΔP, higher fluid resistance, and inferior flow characteristics.

In order to comprehensively assess the influence of the design domain aspect ratio on the flow heat transfer capacity of the heat dissipation channel, the integrated enhanced heat transfer factor PEC based on equal pump power is adopted to evaluate the merits of the enhanced heat transfer capacity of the channel [28], which is expressed by the following equation:

$$PEC = \left(\frac{Nu}{Nu_0}\right) \Big/ \left(\frac{f}{f_0}\right)^{1/3} \tag{20}$$

where Nu and f represent average Nusselt number and Darcy resistance coefficient, respectively. Nu_0 and f_0 are the baseline values of the microchannels which are not topologically optimized for the same laminar flow conditions and the same equivalent diameter.

The variation plot of microchannel PEC with Reynolds number for various design domain aspect ratios is presented in Fig. 10. The figure indicates a declining trend with rising Reynolds number for the combined enhanced heat transfer factor PEC of the five microchannels. The aspect ratio of the design domain affects the PEC of the heat sink under the same Reynolds number condition. The outcome reveals that the PEC of the microchannel is at its maximum at an aspect ratio of 25/64, which further indicates that the enhanced heat transfer capacity of the microchannel is best at this time.

When the flow heat transfer characteristics of each aspect ratio microchannel are compared, it can be seen that the microchannel has the best enhanced heat transfer effect and the best flow heat transfer characteristics at the aspect ratio of 25/64.

6.2.3 Velocity field and temperature field synergy analysis

Professor Guo [19] proposed the field synergy principle after conducting theoretical research on heat transfer processes. He held that the angle of velocity-pressure gradient and velocity-temperature gradient of the fluid, namely, the degree of synergy between the physical fields is closely related to the fluid heat transfer and flow characteristics.

In the fluid flow region, ignoring the axial heat conduction at the fluid inlet and outlet, the

convective heat transfer energy equation is integrated and a dimensionless variable is introduced, then the relationship between the *Nu* and the velocity and temperature field is obtained:

$$Nu_x = Re_x Pr \int_0^1 \left(\overline{U} \cdot \nabla \overline{T}\right) d\overline{y} \tag{21}$$

where *Nu*, *Re* and *Pr* denote the Nusselt number, the Reynolds number and the Prandtl number, respectively.

According to the synergistic relationship between the velocity and temperature fields, the synergistic effect of the two can be evaluated by the field synergy number F_c, whose formula is derived from the above equation (21) as follows:

$$F_c = \int_0^1 \overline{U} \cdot \nabla \overline{T} d\overline{y} = \frac{Nu_x}{Re_x Pr} \tag{22}$$

According to equation (22), when F_c=1, it means that the velocity field is completely synergistic with the temperature field, and the convective heat transfer intensity is at its highest; when F_c=0, it means that the velocity vector direction is perpendicular to the temperature vector direction, and the degree of synergy is at its lowest. In the typical flow heat transfer process, the field synergy number F_c is much less than 1, indicating that the velocity direction is nearly perpendicular to the temperature gradient direction in the actual convective heat transfer process, so the improvement of synergy can be achieved in the optimized design to strengthen the heat transfer purpose.

Fig. 11 presents the correlation of the field synergy number F_c with Reynolds number for different design domain length and width microchannels. As can be seen from the figure, the cooling fluid in the microchannel is in the laminar flow zone, and the field synergy number F_c gradually rises as the Reynolds number rises. This occurs because as the Reynolds number rises, the distribution of fine branch pathways in the channel becomes denser, and the synergy degree between the velocity and temperature fields is enhanced to the point where the synergy degree of heat transfer in the entire channel rises; The F_c of a microchannel with an aspect ratio of 25/64 is the largest under the same Reynolds number and the F_c of a microchannel with a ratio of 64/25 is the smallest; this means that the velocity field and temperature field of a microchannel with an aspect ratio of 25/64 have the best synergistic effect and the best enhanced heat transfer effect is achieved.

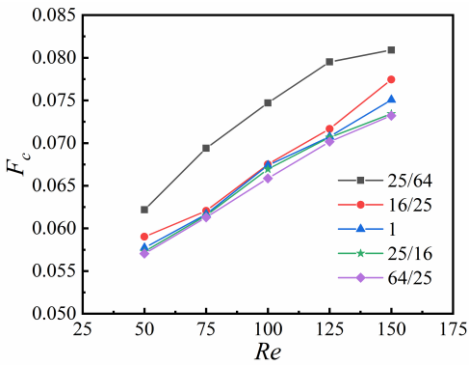

Fig. 11. F_c of the microchannels at different *Re*

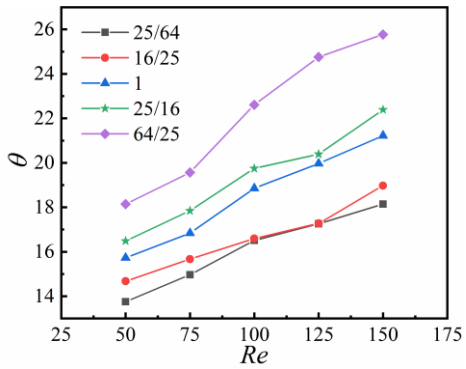

Fig. 12. θ of the microchannels at different *Re*

6.2.4 Velocity field and pressure field synergy analysis

The synergistic relationship between the velocity and the pressure field is expressed as:

$$U \cdot (-\nabla P) = |U||-\nabla P| \cos\theta \tag{23}$$

Thus, the expression of the pressure drop synergy angle can be derived as:

$$\theta = \arccos \frac{U \cdot (-\nabla P)}{|U||-\nabla P|} \tag{24}$$

When $U \cdot (-\nabla P)$ is known, if θ is smaller, the smaller $|U||-\nabla P|$ is, the smaller the power consumption of the equipment, thus the better the synergy of velocity and pressure fields can be obtained; if θ is a fixed value, the smaller $|U||-\nabla P|$ is, the smaller $U \cdot (-\nabla P)$ is, and the smaller the equipment does power. It is apparent that the smaller θ is, the better the synergy of velocity field and pressure field is, the smaller the power consumption is, and the more effectively the goal of energy conservation is served.

Fig. 12 illustrates the correlation of the microchannel pressure drop synergy angle with Reynolds number for different design domain aspect ratios. Due to the degree of fluid disturbance is increased and more drag losses are generated with the increase of Reynolds number, the pressure drop synergy angle θ of microchannel is raised and the synergy effect of velocity and pressure fields of microchannel is decreased with the increase of Reynolds number under the premise of the same aspect ratio. Under the same Reynolds number conditions, as the aspect ratio increases, the fine branch flow on both sides of the main channel gets denser and wider, the flow deterioration area gradually widens, and the pressure drop synergy angle gradually increases. This suggests that the increase in the design domain aspect ratio has a weakening effect on the fluid flow in the microchannel, and the resistance loss of the fluid is increased.

6.2.5 Entransy dissipation analysis

By means of the thermoelectric comparison, a new physical quantity, entransy, was proposed by Guo et al. [20]. The entransy of an object is represented as its heat transfer capacity, as given below：

$$E_{vh} = \frac{1}{2} Q_{vh} U_{vh} = \frac{1}{2} Q_{vh} T \tag{25}$$

where Q_{vh}, U_{vh}, and T are the heat stored for the object, the object thermal potential, and temperature, respectively.

If there is no internal heat source in the heat conduction process, its energy conservation equation can be modified to:

$$\rho c_p U \cdot \nabla \left(\frac{T^2}{2} \right) = \nabla (\lambda T \nabla T) - \lambda |\nabla T|^2 \tag{26}$$

$$U \cdot \nabla (e_{vh}) = \nabla \cdot \left(\dot{e}_h \right) - E_{vh} \tag{27}$$

where e_{vh} is the object entransy dissipation term; $\dot{e}_h$ is the entransy dissipation term of the fluid microelement; E_{vh} represents the entransy dissipation per unit volume in the heat diffusion process, which is as expressed below:

$$E_{vh} = \lambda |\nabla T|^2 \tag{28}$$

The entransy dissipation extremum principle [20] states: the smaller the entransy dissipation value, the better the heat transfer efficiency of the heat sink in the heat conduction process with constant heat flow boundary conditions; the larger the entransy dissipation value, the better the heat transfer efficiency of the heat sink in the heat conduction process with constant temperature boundary conditions.

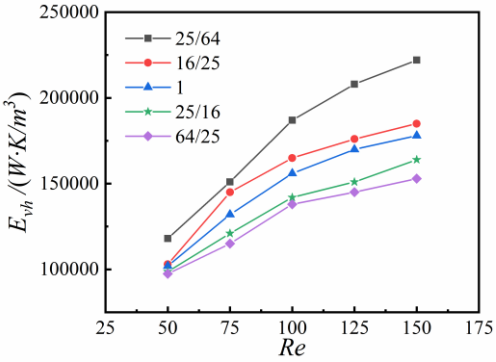

Fig. 13. E_{vh} of the microchannels at different *Re*

The variation of E_{vh} with Reynolds number for microchannels with different design domain aspect ratios is presented in Fig. 13. The figure shows that as the Reynolds number rises, the E_{vh} of the five heat dissipation channels gradually increases. The larger E_{vh} indicates the better heat dissipation effect, according to the extreme value of entransy dissipation principle, when wall temperatures are identical. As a result, for a microchannel with the same aspect ratio, increasing its mass flow rate promotes the fluid perturbation effect to be strengthened. Meanwhile, increasing the branching of the flow paths in the design domain encourages a reduction in the energy dissipation caused by the shunt effect, which in turn increases the convective heat transfer coefficient and enhances heat transfer efficiency. For the same Reynolds number, the E_{vh} increases as the design domain aspect ratio decreases. At lower Reynolds numbers, the design domain has more concentrated high-temperature zones and fewer runner branching structures, which results in poor heat dissipation and an uneven temperature distribution throughout the domain. The main flow path in the domain starts to produce more finely branched flow paths as the Reynolds number gradually increases. As a result, the heat transfer area increases, the convective heat transfer coefficient increases, and the efficiency of heat transfer is improved. When the Reynolds number is higher, the microchannel with the design domain aspect ratio of 25/64 still splits near the inlet side, unlike other microchannels with the same aspect ratio. This causes the resulting fine branch flow paths to be evenly distributed throughout the entire design domain, which gradually increases fluid-solid heat transfer area and successfully prevents the development of localized high-temperature zones in the domain, and the heat transfer effect is enhanced. Therefore, the largest E_{vh} and best heat transfer effect are obtained in the microchannel with the design domain aspect ratio of 25/64, which fulfills the entransy dissipation extremum principle.

7. Conclusion

In this study, the heat dissipation of high heat flow density electronic devices is examined with the bi-objective topology optimization method. Meanwhile, to offer theoretical support for the actual engineering use of microchannels, the optimization strategy of the flow heat transfer process based on the field synergy principle and entransy dissipation theory is also explored, and the following conclusions are drawn.

(1) In the laminar flow state, as the *Re* grows, the number of fine branch channels in the domain rises, the heat transfer area is expanded, the convective heat transfer intensity is enhanced, the flow resistance gradually increases, and the flow characteristics decrease. In addition, for the microchannels with different topologies, the optimal heat transfer performance and the best flow characteristics are

obtained for the microchannel with a design domain aspect ratio of 25/64.

(2) The field synergy principle and entransy dissipation theory are used as the basis for the analysis of optimal heat transfer characteristics. In laminar flow, with the increment of *Re*, the degree of synergy between the velocity and temperature fields is increased by the dense distribution of the finely branched flow channels in the channel, which in turn rises the degree of heat transfer synergy throughout the channel. The F_c and θ of microchannels with various topologies gradually rise as well. This improves the efficiency of heat transfer. The design domain aspect ratio of 25/64 has the largest heat dissipation channel F_c, the smallest pressure drop synergy angle θ, and the largest E_{vh} at the same *Re*, indicating that the velocity-temperature and velocity-pressure fields of the microchannel have the highest degree of synergy, the best heat transfer effect, and the best flow characteristics at this time. It is clear that the enhancement of the heat transfer properties of microchannels can be guided by the field synergy principle and the energy dissipation theory.

Acknowledgement

The authors thank the support of the Postgraduate Quality Improvement Program Project in Shandong Province (SDYAL21159).

Nomenclature

e_{vh}	Object entransy dissipation term	*Greek*	
E_{vh}	Entransy dissipation [kg·m·K/s^3]	α	Inverse permeability
F_c	Field synergy number	β	Projection slope
f	Darcy resistance coefficient	γ	Design variable
PEC	The integrated enhanced heat transfer factor	ρ	Density [kg/m$^{3]}$
T_{ave}	Average temperature [K]	ω	Weighting factor
T_{max}	Maximum temperature [K]	θ	Pressure drop synergy angle [°]

References

[1] O'Connor, P. D. T., Arrhenius and electronics reliability, *Quality and Reliability Engineering International*, 5 (1989), 4

[2] Tuckerman, D. B., Pease, R. F. W., High-performance heat sinking for VLSI, *Ieee Electron Device Letters*, 2 (1981), 5

[3] Adham, A. M., et al., Thermal and hydrodynamic analysis of microchannel heat sinks: A review, *Renewable and Sustainable Energy Reviews*, 21 (2013)

[4] Lin, Z., et al., Heat transfer augmentation characteristics of a fin punched with curve trapezoidal vortex generators at the rear of tubes, *Thermal Science*, 26 (2022), 4B, pp. 3529-3544

[5] Deng, D., et al., Experimental and numerical study of thermal enhancement in reentrant copper microchannels, *International Journal of Heat and Mass Transfer*, 91 (2015)

[6] Zhu, Q., et al., Effects of geometric parameters on fluid-flow and heat transfer in micro-channel heat sink with trapezoidal grooves in sidewalls, *Thermal Science*, 26 (2022), 4B, pp. 3641-3651

[7] Fang, Y., et al., Numerical study on heat and flow transfer characteristics in rectangular mini-channel with S-shaped turbulator inserted, *Thermal Science*, 00 (2022), p. 210-210

[8] Ansari, D., Kim, K., Performance Analysis of Double-Layer Microchannel Heat Sinks under Non-Uniform Heating Conditions with Random Hotspots, *Micromachines*, 8 (2017), 2

[9] Lei, Y., et al., Computational and experimental investigation of condensation flow patterns and heat transfer in parallel rectangular micro-channels, *International Journal of Heat and Mass Transfer*, 149 (2020), C
[10] Wei, J., et al., Heat Transfer Enhancement by Sinusoidal Wavy Tape Insert in Two-pass Ribbed Channels, *Thermal Science*, 26 (2022), 6A, pp. 4657-4668
[11] Hiep, H. C., et al., Impact of fin geometry and surface roughness on performance of an impingement two-phase cooling heat sink, *Applied Thermal Engineering*, 198 (2021)
[12] Philip, B. M., Noboru, K., Generating optimal topologies in structural design using a homogenization method, *Computer Methods in Applied Mechanics and Engineering*, 71 (1988), 2
[13] Borrvall, T., Petersson, J., Topology optimization of fluids in Stokes flow, *International Journal for Numerical Methods in Fluids*, 41 (2003), 1
[14] Guanghui, W., et al., Design and performance enhancement of thermal-fluid system based on topology optimization, *Applied Mathematical Modelling*, 116 (2023)
[15] Yaji, K., et al., Topology optimization in thermal-fluid flow using the lattice Boltzmann method, *Journal of Computational Physics*, 307 (2016)
[16] Yang, X., et al., Numerical investigation of microchannel heat sinks with different inlets and outlets based on topology optimization, *Applied Energy*, 330 (2023), PA
[17] Zhang, M., et al., Numerical simulation and analysis of lithium battery heat dissipation based on multi-objective optimization, *Thermal Science* (2022), 00, p. 208-208
[18] Anqi, Z., et al., Topology optimization for a water-cooled heat sink in micro-electronics based on Pareto frontier, *Applied Thermal Engineering*, 207 (2022)
[19] Guo, Z. Y., et al., The field synergy (coordination) principle and its applications in enhancing single phase convective heat transfer, *International Journal of Heat and Mass Transfer*, 48 (2005), 9, pp. 1797-1807
[20] Guo, Z., et al., Entransy—A physical quantity describing heat transfer ability, *International Journal of Heat and Mass Transfer*, 50 (2007), 13/14
[21] Ting, Z., et al., Topology optimization of regenerative cooling channel in non-uniform thermal environment of hypersonic engine, *Applied Thermal Engineering*, 219 (2023), PA
[22] Matsumori, T., et al., Topology optimization for fluid–thermal interaction problems under constant input power, *Structural and Multidisciplinary Optimization*, 47 (2013), 4
[23] Stolpe, M., Svanberg, K., An alternative interpolation scheme for minimum compliance topology optimization, *Structural and Multidisciplinary Optimization*, 22 (2001), 2
[24] Fridolin, O., Henrik, B., Scaling behavior of optimally structured catalytic microfluidic reactors., *Physical Review. E, Statistical, Nonlinear, and Soft Matter Physics*, 75 (2007), 1 Pt 2
[25] Lazarov, B. S., Sigmund, O., Filters in topology optimization based on Helmholtz- type differential equations, *International Journal for Numerical Methods in Engineering*, 86 (2011), 6
[26] Jianhong, Z., et al., Thermal design of microchannel heat sinks using a contour extraction based on topology optimization (CEBTO) method, *International Journal of Heat and Mass Transfer*, 189 (2022)
[27] Fan, J. F., et al., A performance evaluation plot of enhanced heat transfer techniques oriented for energy-saving, *International Journal of Heat and Mass Transfer*, 52 (2009), 1/2

Submitted: 01.07.2023.
Revised: 14.09.2023.
Accepted: 16.09.2023.